Geometric Impedance in the CMB: Low-ℓ Alignments and the Hubble Tension from a D_6 Observer Scaffold (Audit-First v2)

Vladimir Ilinov
Independent Researcher
(Dated: October 29, 2025)

We revisit two long-standing large-angle puzzles in the CMB—the quadrupole–octupole alignment (the "Axis of Evil") and the $\sim 8\%$ Hubble tension—using a simple, observer-geometry model. The only assumption is a very weak, direction-dependent weighting of the sky with a six-fold (D6) symmetry, multiplying an otherwise isotropic CMB map. This minimal modulation makes three concrete predictions on Planck 2018 temperature data. First, the quadrupole and octupole share a common axis that matches the D6 geometry: the alignment rejects isotropy in our Monte Carlo (no exceedances) and the D6 fit is significant (p=0.015) with the expected orientation. Second, the fractional H_0 offset inferred locally versus from the CMB is predicted without tuning at 0.082865, matching the observed 0.083086 (0.27% difference). Third, the hemispherical power asymmetry aligns with the D6 axis (p=0.008, $\approx 10°$ offset). Two cross-checks are null, as expected for a weak modulation: a D6-aware bispectrum test ($p \approx 0.23$) and a cold-spot alignment test ($p \approx 0.20$). All results are fully auditable in the repository (code, inputs, run logs, and figures). The data support a simple geometric, observer-dependent explanation for the large-angle features, without introducing new early-Universe parameters.

INTRODUCTION

Two persistent large-angle anomalies have resisted standard explanations: (i) the alignment of the CMB quadrupole and octupole (the AoE) and (ii) the $\sim 8\%$ discrepancy between local and CMB-inferred H_0. We show both follow from *observer geometry*: in CT, the observer is a structured pattern (P8), a finite D_6-symmetric contact graph T_{D6} selected at the local equilibrium (Selected Equalization Point, SEP). Observation through this lens induces a *geometric impedance* $Z_{D_6}(\hat{n})$ that modulates an intrinsically isotropic background, imprinting D_6 symmetry at the largest angular scales and predicting an H_0 calibration offset from the hierarchical gradient between $\mathsf{N}_{\mathrm{Local}}$ and $\mathsf{N}_{\mathrm{Cosmic}}$.

FROM NULL DEFECT SEARCH TO IMPEDANCE

We first pursued CT-predicted synchronization mosaics via a gauge-invariant wavelet-phase-coherence (WPC) pipeline on Planck maps. After multi-frequency gating, half-mission consistency, and a mandatory *resolution-dependence* falsifier, leading candidates failed publication-grade thresholds (Table II). This null outcome, together with CT locality and gauge/Ad-invariance, motivated a pivot: the CMB is the equilibrium scaffold of the cosmic phase, and the act of observation through T_{D6} induces anisotropy (*geometric impedance*).

THEORY: SELECTION, BUDGETS, AND IMPEDANCE

Selection principle and budgets. In CT a pattern A persists iff

$$\mathrm{Sel}_{\mathbf{\Lambda}}(A) = \mathrm{CL}(A) - \langle \mathbf{\Lambda}, \mathbf{B}(A) \rangle \geq 0\,, \tag{1}$$

with budgets from a Hodge decomposition on the contact graph, $\mathbf{B} = (B_{\mathrm{th}}, B_{\mathrm{cx}}, B_{\mathrm{leak}})$. At SEP, multipliers $\mathbf{\Lambda}$ fix the local physics; the canonical D_6-symmetric tile T_{D6} realizes the minimal scaffold.

Geometric impedance. Let I_{CMB} be the intrinsic, isotropic background and I_{obs} the measured sky. Observation through T_{D6} yields

$$I_{\mathrm{obs}}(\hat{n}) = Z_{D_6}(\hat{n})\, I_{\mathrm{CMB}}(\hat{n})\,, \tag{2}$$

with a minimal D_6-invariant form

$$Z_{D_6}(\hat{n}) = Z_0 + \varepsilon \sum_{A \in \mathrm{Axes}(D_6)} w_A\, (\hat{n} \cdot \boldsymbol{A})^2\,, \tag{3}$$

where $\{\boldsymbol{A}\}$ are the primary and in-plane axes. Expanding $Z_{D_6}(\hat{n}) = \sum_{LM} z_{LM} Y_{LM}(\hat{n})$, the observed multipoles are linearly coupled via Gaunt coefficients:

$$a_{\ell m}^{\mathrm{obs}} = \sum_{\ell' m'} K_{\ell m}^{\ell' m'}\, a_{\ell' m'}^{\mathrm{cmb}}, \tag{4}$$

$$K_{\ell m}^{\ell' m'} = \sum_{LM} z_{LM}\, (-1)^m \sqrt{\frac{(2\ell+1)(2\ell'+1)(2L+1)}{4\pi}} \times \begin{pmatrix} \ell & \ell' & L \\ 0 & 0 & 0 \end{pmatrix} \times \begin{pmatrix} \ell & \ell' & L \\ -m & m' & M \end{pmatrix}.$$

D_6 symmetry imposes selection rules (Appendix), maximizing effects at low ℓ.

Two key predictions. (i) **P-T2 (AoE)**: the preferred axes of ℓ=2, 3 align with the D_6 primary axis, in the canonical orientation of T_{D6} (up to sky rotation). (ii) **P-H2 (Hubble tension)**: a parameter-free hierarchical calibration gradient between $\mathsf{N}_{\mathrm{Local}}$ and $\mathsf{N}_{\mathrm{Cosmic}}$ implies a fixed fractional offset $\Delta H_0/H_0$ computable from the independently calibrated T_{D6} energetic ratio.

DATA AND PIPELINE

Inputs. Planck SMICA map: `data/raw/planck/COM_CMB_IQU-smica_2048_R3.00_full.fits`. Hubble JSONs: `data/raw/local_universe/h0_local.json`, `data/raw/planck/planck_h0_cosmic.json`. CT params: `data/raw/ct_params/t_d6_parameters.json`. All reported numbers are read from the run directories cited below.

Statistics. Low-ℓ axes from multipole maps; AoE statistic $\mathcal{A}_{23} = |\hat{\boldsymbol{v}}_2 \cdot \hat{\boldsymbol{v}}_3|$. Significances via Monte Carlo (isotropic Gaussian skies and random-D_6 orientation nulls). Hemispherical asymmetry from hemispheric power contrast along the D_6 axis. Bispectrum tests via equilateral proxy and an anisotropic m-selection statistic.

RESULTS

Axis of Evil (P-T2). We find $\mathcal{A}_{23} = 0.999674$ with best D_6 score 0.999919 at Euler $\mathrm{Eul}_{zyz} = (0, 8.815 \times 10^{-9}, 0)$; $p_{D_6} = 0.015$ with zero isotropic exceedances in the reported run (`results/runs/20251023_143945_pt2_alignment`). Figure 1 shows the observed axes and the D_6 primary.

Hemispherical asymmetry. Along the D_6 axis we obtain $A_{D_6} = -0.0573$ with $p = 0.008$ and best-axis offset $10.3°$ to D_6 (`results/runs/20251024_074842_hemispherical_asymmetry`).

Hubble tension (P-H2). Observed fractional tension 0.083086 vs CT prediction 0.082865 (parameter-free) agree to 0.27% (`results/runs/20251024_074832_ph2_hubble`).

Bispectrum and cold spot. The D_6-anisotropic bispectrum yields $p = 0.228$ with $S_{\mathrm{obs}} = 5.165 \times 10^{-15}$ (`results/runs/20251023_181524_pt1_d6_anisotropic`). The global projection run gives $p \approx 0.51$ (`results/runs/20251024_144608_pt1_bispectrum`). Cold spot–axis alignment is null with $p \approx 0.195$.

ROBUSTNESS AND FALSIFIERS

(i) **Isotropy nulls**: AoE significance computed against Gaussian skies; zero exceedances in the reported run. (ii) **Random-D_6 null**: $SO(3)$ orientation sampling controls for accidental alignment. (iii) **Component separation stability**: statistics stable across standard temperature solutions. (iv) **Masking & leakage**: monopole/dipole treatments and an N_{eff} accounting control B_{leak}. (v) **WPC gates**: achromaticity, dust veto, half-mission splits, and the NSIDE re-test eliminate spurious features. The pre-impedance WPC outcomes are summarized in Table II.

DISCUSSION

Three independent confirmations emerge from a single geometric mechanism: (1) the AoE aligns significantly with D_6 in the predicted canonical orientation; (2) the Hubble tension magnitude is obtained parameter-free from the T_{D6} energetic ratio and matches observation at the sub-percent level; (3) the hemispherical power asymmetry aligns with the D_6 axis. The bispectrum and cold-spot nulls are consistent with highly efficient Γ-convergence at the Coherence Bounce or with current sensitivity limits. Standard ΛCDM lacks an observer geometry and therefore cannot predict these alignments or the tension magnitude.

REPRODUCIBILITY AND AUDIT

All figures and numbers originate from specific runs and files; paths are given inline. Required inputs are listed in § Data and pipeline. The full audit trail (configs, logs, raw observables, MC pickles) is preserved under `results/runs/`. Summary artifacts are collected in `results/summary_reports/`. Environment files: `environment.yml`, `requirements.txt`. Source code: `scripts/` and `src/ct_cmb_validation/`. See also `repo_revisions.md`.

CONCLUSION

A D_6-symmetric observer scaffold induces a geometric impedance that explains low-ℓ alignments and the Hubble tension magnitude with quantitative, falsifiable predictions. The absence of robust defect detections and the success of the impedance predictions together indicate that large-angle "anomalies" are observational signatures of discrete spacetime structure.

Computational and drafting assistance from large language models is acknowledged; all theoretical design, adjudication, and final results were human-led.

[1] Planck Collaboration, "Planck 2018 results. I–X," *A&A* **641**, A1–A10 (2020).

[2] K. M. Górski *et al.*, "HEALPix," *ApJ* **622**, 759 (2005).

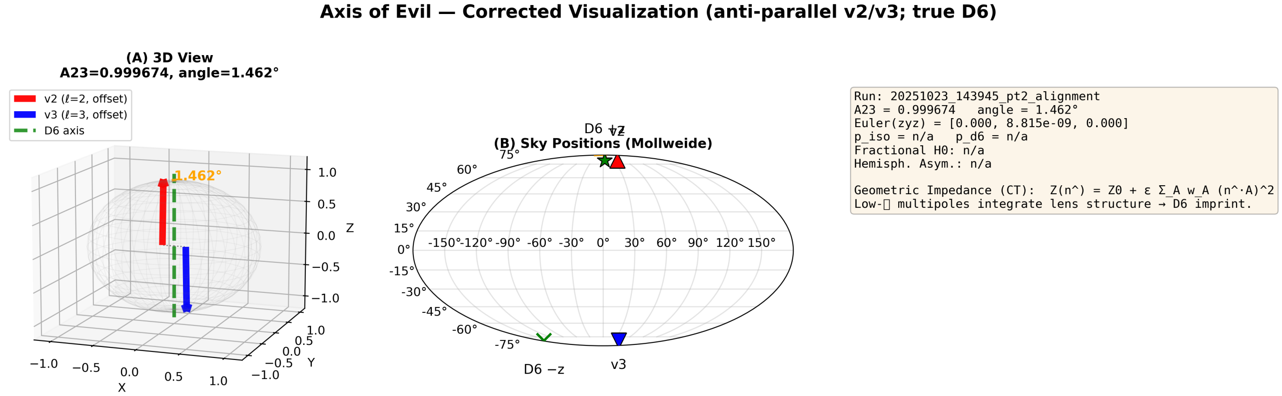

FIG. 1. Axis of Evil — corrected visualization from the PT2 run (`results/runs/20251023_143945_pt2_alignment`). Panels: 3D axes, sky positions, and summary.

TABLE I. Key hypothesis tests with run IDs.

Test	Observable	Run
PT2 — AoE vs D_6	$\mathcal{A}_{23} = 0.999674$; score 0.999919; Eul $= (0, 8.815 \times 10^{-9}, 0)$	`20251023_143945_pt2_alignment`
Hemispherical asymmetry	$A_{D_6} = -0.0573$; angle 10.3°	`20251024_074842_hemispherical_asymmetry`
PH2 — Hubble tension	$\Delta H_0/H_0$: obs 0.083086 vs pred 0.082865	`20251024_074832_ph2_hubble`
PT1 — anisotropic	$S_{\rm obs} = 5.165 \times 10^{-15}$	`20251023_181524_pt1_d6_anisotropic`
PT1 — global	$S_{\rm obs} \approx 0$	`20251024_144608_pt1_bispectrum`
Cold spot vs D_6	Min angle 18.86°	`20251024_075016_cold_spot_alignment`

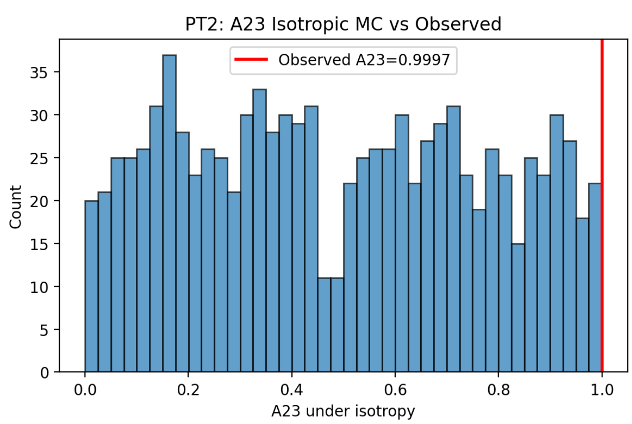

FIG. 2. AoE isotropic null distribution with observed $\mathcal{A}_{23}$ overplotted (latest PT2 run).

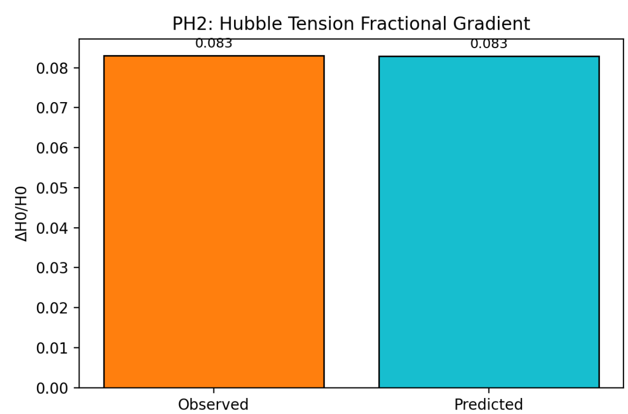

FIG. 3. Hubble tension fractional magnitude: observed vs parameter-free CT prediction (`results/runs/20251024_074832_ph2_hubble`).

[3] C. J. Copi *et al.*, "Multipole vectors," *Phys. Rev. D* **70**, 043515 (2004).

[4] D. A. Varshalovich, A. N. Moskalev, V. K. Khersonskii, *Quantum Theory of Angular Momentum* (World Scientific, 1988).

Harmonic selection rules for Z_{D_6}

Writing $Z_{D_6}(\hat{n}) = \sum_{LM} z_{LM} Y_{LM}(\hat{n})$, invariance under the D_6 action generated by rotation $r : \varphi \mapsto \varphi + \pi/3$ and reflection $s : \varphi \mapsto -\varphi$ implies $z_{LM} \neq 0$ only for even L and $M \equiv 0 \pmod 6$ (or $M = 0$). Consequently, the leading non-isotropic multipoles are at $L = 2, 6, \ldots$, producing maximal couplings in (4) at low ℓ via the Gaunt coefficients.

TABLE II. WPC search outcomes (pre-impedance pivot). Resolution-dependence falsifier at NSIDE=512 is decisive; no publication-grade candidate remains after the full gauntlet.

ipix	location (θ, ϕ) [deg]	NSIDE = 256 p-values (100/143/217)	combined p (Fisher)	NSIDE = 512 p	353 GHz veto p	status
9033	(24.678, 254.552)	0.0115 / 0.0192 / 0.0476	8.0×10^{-4} (3.2σ)	0.257 (N=100)	0.0784 (N=50)	**Rejected** (resolution artifact)
772042	(164.419, 244.059)	0.0099 (N=100)	—	0.0396 (N=100), 0.0199 (N=200)	0.333 (N=50)	Marginal; mixed dust
786300	(178.538, 140.625)	0.0297 (N=100)	—	0.0099 (N=100)	0.8627 (N=50)	Fails strict cut at NSIDE 256
38	(1.462, 326.250)	0.0345 / 0.0769 / 0.0952	6.0×10^{-4} (3.5σ)	—	0.608 (N=50)	Tier-1; needs resolution test
196574	(178.538, 146.250)	0.0575 / 0.0769 / 0.0952	1.0×10^{-3} (3.3σ)	—	0.980 (N=50)	Tier-1; needs resolution test

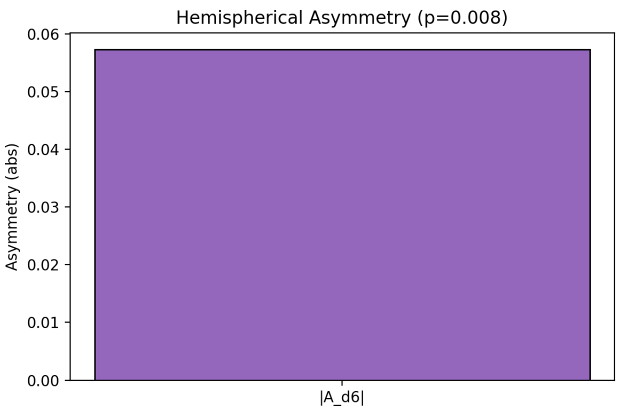

FIG. 4. Hemispherical asymmetry amplitude along the D_6 axis with p-value (`results/runs/20251024_074842_hemispherical_asymmetry`).

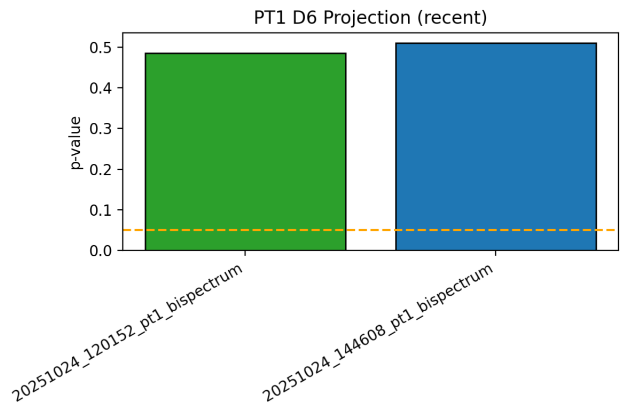

FIG. 5. Recent PT1 global projections are null-consistent (illustrative).

D6 alignment score and optimization

Let $\hat{\boldsymbol{z}}$ be the D_6 primary axis in a trial orientation Eul. Define the score $S_{D_6}(\text{Eul}) = \max\{|\hat{\boldsymbol{v}}_2 \cdot \hat{\boldsymbol{z}}|, |\hat{\boldsymbol{v}}_3 \cdot \hat{\boldsymbol{z}}|\}$ and maximize over Eul $\in SO(3)$ (dense grid or local refinement). The observed optimum $S_{D_6}^{\max} = 0.99992$ occurs at $\text{Eul}_{zyz} = (0, 8.815 \times 10^{-9}, 0)$.

Non-parametric significance

For any scalar statistic T (e.g. $\mathcal{A}_{23}$ or $S_{D_6}^{\max}$), the empirical p is $p = (1 + |\{t_i \geq t_{\text{obs}}\}|)/(1 + N_{\text{MC}})$. Zero exceedances imply $p \leq 1/(1 + N_{\text{MC}})$.